Experimental Verification of Plasmonic Cloaking at Microwave Frequencies with Metamaterials

Brian Edwards,[1] Andrea Alù,[1,2] Mário G. Silveirinha,[1,3] and Nader Engheta[1,*]

[1]*Department of Electrical and Systems Engineering, University of Pennsylvania, Philadelphia, Pennsylvania 19104, USA*
[2]*Department of Electrical and Computer Engineering, University of Texas at Austin Austin, Texas 78712, USA*
[3]*Department of Electrical Engineering, Universidade de Coimbra–Instituto de Telecomunicações, Portugal*

(Received 17 June 2009; revised manuscript received 7 September 2009; published 6 October 2009)

Plasmonic cloaking is a scattering-cancellation technique based on the local negative polarizability of metamaterials. Here we report its first experimental realization and measurement at microwave frequencies. An array of metallic fins embedded in a high-permittivity fluid has been used to create a metamaterial plasmonic shell capable of cloaking a dielectric cylinder, yielding over 75% reduction of total scattering width.

DOI: 10.1103/PhysRevLett.103.153901 PACS numbers: 42.82.Et, 52.40.Db, 52.40.Fd, 78.66.Sq

Throughout history, invisibility and cloaking have always fascinated humanity, yielding hundreds of legends and novels based on the dream of being undetectable. The numerous applications that may benefit from scattering reduction are obvious in just about any frequency range from few MHz to the visible and UV. The recent advances in nanotechnology and metamaterial technology have fostered a strong interest in the possibility of realizing man-made cloaks, and several possibilities and techniques have been put forward in the literature, exploiting the anomalous electromagnetic properties of metamaterials [1–16]. The transformation-based cloaking techniques [1–11] offer the possibility to bend the impinging electromagnetic rays around a specific region, theoretically suppressing any scattering from whatever object is placed inside the cloak. An experimental verification of this cloaking technique at microwave frequencies has been recently reported [2], with an imperfect scattering reduction due to technological limitations.

Although transformation-based cloaking is mathematically elegant and would in principle allow perfect cloaking independent of the source of illumination and the size and nature of the object to be cloaked, its stringent requirements on both the anisotropy and inhomogeneity of the shell, its sensitivity to the design parameters, and the technological challenges associated with its realization have proven to make this cloaking technique challenging for higher frequency ranges such as IR and optical domains. Indeed, the geometric variations which created the required inhomogeneity in Ref. [2] were as subtle as 0.018% of the free-space wavelength which is both a testament to the excellent quality of the work in [2] and the complexity of the technique. Transformation-based cloaking is the appropriate and useful technique for a class of problems in which the wavelength is much larger than the smallest manufacturable feature and the object is larger than the wavelength. However, there remains a large class of problems in which the critical dimension of the object is comparable with the wavelength of operation and fabricating features orders of magnitude below this is not trivial, particularly in the optical domain.

In 2005, we suggested a different route to invisibility cloaking based on the scattering-cancellation properties of plasmonic materials with low positive or negative permittivity [17–24]. In some sense related to earlier quasistatic theoretical works on metallic nanoparticles [25], we have shown that moderately sized dielectric or conducting objects may be effectively cloaked with a simple homogeneous and isotropic layer of plasmonic material. In this case, the wave can penetrate through the cloak and the effect is associated with the out-of-phase scattering properties of plasmonic materials. We have later extended these concepts to collections of particles [20], multifrequency operation [21], larger sized objects [24], highlighting also the robustness, relatively less narrower bandwidth of operation, and simplicity of this alternative route to invisibility [19].

Because of its overall simplicity, the realization of a plasmonic cloak may follow several routes. Homogenous and isotropic plasmonic shells are already available in nature at infrared and optical frequencies in the form of polar dielectrics and noble metals. Additionally, metamaterials with low positive or negative effective permittivity may be realized at lower frequencies. As an example, we have envisioned a simple design for a metamaterial plasmonic cloak operating at microwave frequencies [18] based on earlier works on the effective electromagnetic properties of metamaterials composed of parallel metallic fins [26]. As we have theoretically shown [18], a cylindrical plasmonic shell as depicted in Fig. 1(a) may be well characterized by an effective permittivity $\varepsilon_{\text{cloak}}$ given by

$$\varepsilon_{\text{cloak}} = \varepsilon_{\text{diel}} - \frac{N^2/4}{k_0^2 r_{\text{inner}} r_{\text{outer}}}, \tag{1}$$

where N is the number of metallic fins, $k_0 = \omega/c$ is the free-space wave number, $\varepsilon_{\text{diel}}$ is the relative permittivity of the material surrounding the inclusions, and r_{inner} and r_{outer} are the inner and outer boundaries of layer. It is evident

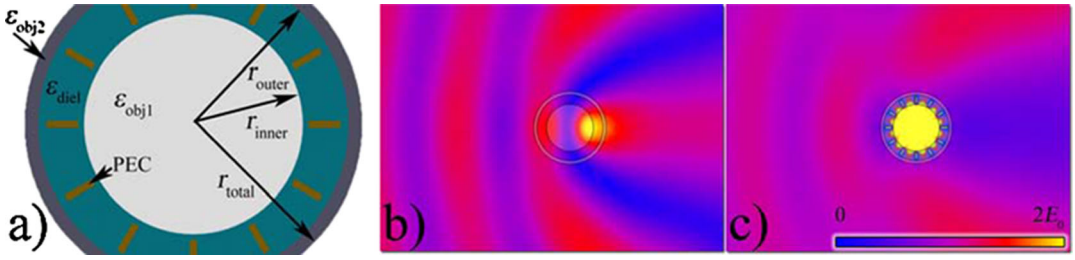

FIG. 1 (color online). Numerical simulations. (a) Object and cloak geometry. (b) Numerical simulation of the uncloaked object at the design frequency examining the magnitude of the electric field normal to the cross-section plane. (c) Numerical simulation of the cloaked object at the same frequency.

that, after proper design, ε_{cloak} may be tailored to become low positive or negative, as required for obtaining scattering cancellation with plasmonic cloaking [17].

Here we report the first experimental verification of these concepts, obtained at microwave frequencies. The object to be cloaked consists of a dielectric cylinder with large permittivity and moderate size. For practical purposes, a plastic shell with small permittivity contrast compared to the background is also added for structural support of the constructed prototype, as explained below. As we have thoroughly verified, the presence of the plastic shell affects only very minorly the scattering properties of the dielectric cylinder, and it may be neglected for practical purposes. When illuminated by a TEM wave generated in the far-field of the object, the total electric field distribution, as simulated with finite-integration technique commercial software [27], is shown in Fig. 1(b). As expected, there is a significant shadow behind and standing wave in front of the object, produced by a relatively large amount of scattering from the central cylinder. In contrast, by replacing the air gap with a metamaterial-based plasmonic layer, carefully designed [18] to achieve the desired effective permittivity ε_{cloak} and thickness, we see substantially decreased scattering. This is shown by the better uniformity of the wave in numerical simulation of Fig. 1(c) [17–24], indicating that the shadow behind and reflected wave in front of the object has been reduced by the cloak. It is relevant to note that this cloaking effect is obtained by inserting a high-contrast liquid (acetone) and regularly spaced metallic fins in the region between the shell and the object, which by themselves may be expected to produce strong scattering.

The experimental setup with which we have tested these concepts is depicted in Fig. 2. Since the geometry of interest is two-dimensional and independent of the cylinder axis, the experimental apparatus consists of a finite cylinder placed inside a parallel plate waveguide supporting only the fundamental TEM mode. The lower plate consists of the metallic surface of an optical table, while the upper plate is a perforated aluminum sheet, with a separation of 50.8 mm from the bottom plate. The sides of the parallel plate waveguide are ringed with carbon impregnated absorbing material to simulate infinite extents. The uncloaked object consists of a plastic rod ($r_{inner} = 19$ mm) with $\varepsilon_{obj1} = 6.0$ surrounded by a plastic shell ($r_{outer} = 27$ mm and $r_{total} = 31.3$ mm) with $\varepsilon_{obj2} = 2.6$, which is necessary for structural support. It is emphasized that the plastic shell only negligibly affects the scattering properties of the system. For the cloaked object, the space between the plastic rod and shell is filled with acetone $\varepsilon_{diel} = 21$ and $N = 12$ metallic inclusions, yielding an effective permittivity $\varepsilon_{cloak} = -22$ at the design frequency

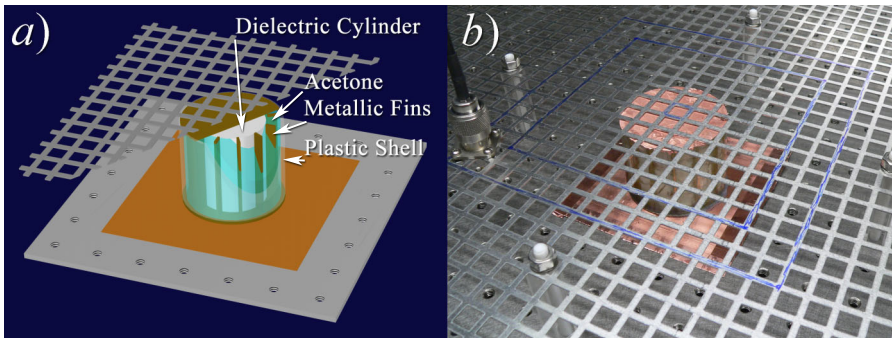

FIG. 2 (color online). Experimental setup. (a) Schematic model showing the cloaked object consisting of the dielectric cylinder surrounded by acetone and metallic fins. A plastic shell contains the acetone. The structure is within a parallel plate waveguide. (b) Photograph of the experimental setup with the same cloaked object and the sensing probe used to take the measurements of the local electric field E_z around the square of interest.

of 1.93 GHz. For the uncloaked object this space is filled by air.

In order to quantitatively measure the total scattering reduction achieved by the cloak, we have evaluated the total scattering cross-sectional width in the uncloaked and cloaked scenario. The scattering gain, defined as the ratio between the cloaked and uncloaked scattering widths as a function of frequency is reported in Fig. 3 for the experimental data, full-wave simulations, and analytical calculations [18].

The analytical scattering cross-sectional width in the curves in Fig. 3 is defined as [18]:

$$\mathrm{SCS} = \frac{4}{k_0}\sum_{l=0}^{\infty}(2-\delta_{l,0})|c_l|^2, \qquad (2)$$

where c_l are the Mie scattering coefficients and $\delta_{l,0}$ is the Kronecker delta function. The scattering linewidth, SCS, is the scattered power per unit of (axial) length of cylinder divided by the power flux density (Poynting vector) of the incoming wave.

In order to measure the numerical and experimental scattering cross-sectional widths in Fig. 3, we have selected 52 distinct points on a mathematical square surrounding the cylinder under test. Four measurements were taken around each point through the perforations in the upper aluminum plate of the waveguide (see Fig. 2) with a near-field probe that measures the local electric field normal to the plate. These measurements were performed first for the incident field (without object, E_z^{inc}), then for the uncloaked object ($E_z^{\mathrm{uncloaked,tot}}$), and finally for the cloaked object ($E_z^{\mathrm{cloaked,tot}}$). The quantities $E_z^{\mathrm{uncloaked,scat}} = E_z^{\mathrm{uncloaked,tot}} - E_z^{\mathrm{inc}}$ and $E_z^{\mathrm{cloaked,scat}} = E_z^{\mathrm{cloaked,tot}} - E_z^{\mathrm{inc}}$ were then calculated over the whole range of frequencies

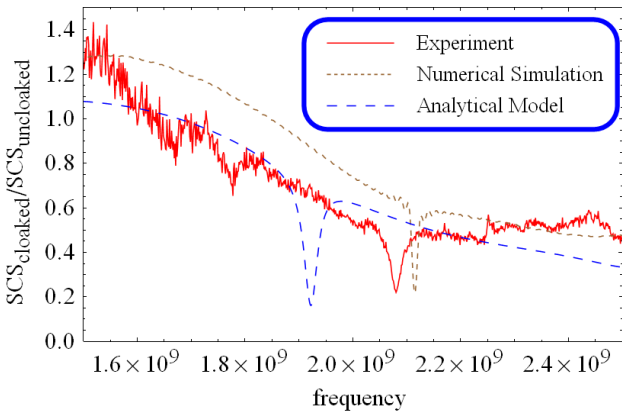

FIG. 3 (color online). Plot of the ratio between the scattering cross-section widths for the cloaked and uncloaked objects. Red or solid line: postprocessed experimental result; brown or short-dashed line: numerical simulation of the identical structure; blue or long-dashed line: analytical model of the structure following [18]. The small discrepancy may be associated with deviations from the expected value of permittivity of the acetone and/or due to the finite thickness of fins.

of interest. The full animations are shown in Ref. [28] for both the cloaked and uncloaked cases. The overall relevant scattering reduction is evident in these animations.

The total scattering width was then determined by retrieving the transverse components of the magnetic fields H_x and H_y through the finite spatial derivatives $\partial_y E_z$ and $\partial_x E_z$, respectively. The time averaged components of the real part of the Poynting vector were found through $P_x = -(1/2)E_z H_y^*$ and $P_y = (1/2)E_z H_x^*$. Finally, its outward component was integrated around the square and divided by the average incident power to yield the uncloaked and cloaked scattering widths, respectively, whose ratio is plotted in Fig. 3.

We notice that over a relatively wide range of frequency the scattering gain is less than one, despite the addition of highly scattering materials to the setup in the cloaked scenario. Consistent with our theory [17], this is due to the fact that a plasmonic shell with effectively low positive or negative permittivity scatters a wave that is out of phase with the one produced by the original dielectric object, allowing an overall scattering reduction for the system as a whole.

It is noticed that around the design frequency, at approximately 2 GHz, the scattering gain curves take a dramatic dip. This is the frequency at which the dominant scattering orders (azimuthally symmetric) from the cloak and the object cancel out, leaving only some small residual scattering associated with higher-order multipoles. There is a small discrepancy between the location of the dip in the analytical curve compared with the simulation and experimental curves. This might be mainly attributed to the 1.25 mm thickness of the metallic fins that was not modeled in our original theory [18] and with small variations in the acetone permittivity. Regardless, in all curves in Fig. 3 there is a significant reduction in the scattering cross-section width, of approximately 75%.

For smaller objects, whose scattering is largely dominated by the zeroth order scattering multipole, with weaker contributions from residual higher-order scattering multipoles, this reduction would be expected to be even more dramatic. It should be mentioned, moreover, that better performance, even for relatively larger objects [24], might possibly be achieved by adding some degrees of freedom in the cloak design such as multilayered cloaks [21].

As evident from the simulated field plot in Fig. 1(c), the electromagnetic wave indeed is free to penetrate the cloak geometry and enter the dielectric object, a property typical of this plasmonic cloaking technique. This property provides relatively broad bandwidths of operation [24] as confirmed by the experimental results in Fig. 3. Additionally, this feature may open the possibility to noninvasive probing and ''cloaked sensors'' [29].

Most importantly, the underlining simplicity of the design of this plasmonic cloak, which indeed achieves substantial scattering reduction with relatively simple

metamaterial technology, may be easily translated to infrared and optical frequencies, paving the way to a possible experimental realization at higher frequencies.

*Author to whom correspondence should be addressed. engheta@ee.upenn.edu

[1] J. B. Pendry, D. Schurig, and D. R. Smith, Science **312**, 1780 (2006).
[2] D. Schurig *et al.*, Science **314**, 977 (2006).
[3] S. A. Cummer, B. I. Popa, D. Schurig, D. R. Smith, and J. B. Pendry, Phys. Rev. E **74**, 036621 (2006).
[4] W. Cai, U. K. Chettiar, A. V. Kildishev, and V. M. Shalaev, Nat. Photon. **1**, 224 (2007).
[5] W. Cai, U. K. Chettiar, A. V. Kildishev, and V. M. Shalaev, Opt. Express **16**, 5444 (2008).
[6] W. Cai, U. K. Chettiar, A. V. Kildishev, G. W. Milton, and V. M. Shalaev, Appl. Phys. Lett. **91**, 111105 (2007).
[7] U. Leonhardt, Science **312**, 1777 (2006).
[8] U. Leonhardt, New J. Phys. **8**, 118 (2006).
[9] H. Chen, X. Jiang, and C. T. Chan, Phys. Rev. B **76**, 241104 (2007).
[10] M. Yan, Z. Ruan, and M. Qiu, Phys. Rev. Lett. **99**, 233901 (2007).
[11] Z. Ruan, M. Yan, C. W. Neff, and M. Qiu, Phys. Rev. Lett. **99**, 113903 (2007).
[12] G. W. Milton and N. A. Nicorovici, Proc. R. Soc. A **462**, 3027 (2006).
[13] G. W. Milton, N. A. Nicorovici, R. C. McPhedran, and V. A. Podolskiy, Proc. R. Soc. A **461**, 3999 (2005).
[14] A. Greenleaf, Y. Kurylev, M. Lassas, and G. Uhlmann, Commun. Math. Phys. **275**, 749 (2007).
[15] P. S. Kildal, A. A. Kishk, and A. Tengs, IEEE Trans. Antennas Propagat. **44**, 1509 (1996).
[16] P. Alitalo, O. Luukkonen, L. Jylhä, J. Venermo, and S. A. Tretyakov, IEEE Trans. Antennas Propag. **56**, 416 (2008).
[17] A. Alù and N. Engheta, Phys. Rev. E **72**, 016623 (2005).
[18] M. G. Silveirinha, A. Alù, and N. Engheta, Phys. Rev. E **75**, 036603 (2007).
[19] A. Alù and N. Engheta, Opt. Express **15**, 3318 (2007).
[20] A. Alù and N. Engheta, Opt. Express **15**, 7578 (2007).
[21] A. Alù and N. Engheta, Phys. Rev. Lett. **100**, 113901 (2008).
[22] M. G. Silveirinha, A. Alù, and N. Engheta, Phys. Rev. B **78**, 075107 (2008).
[23] A. Alù and N. Engheta, J. Opt. A **10**, 093002 (2008).
[24] A. Alù and N. Engheta, Phys. Rev. E **78**, 045602(R) (2008).
[25] M. Kerker, J. Opt. Soc. Am. **65**, 376 (1975).
[26] W. Rotman, IRE Trans. Antennas Propag. **10**, 82 (1962).
[27] CST Microwave Studio 2008.
[28] See EPAPS Document No. E-PRLTAO-103-013942 for animations of the collected data showing total and scattered fields for the cloaked and uncloaked cases. For more information on EPAPS, see http://www.aip.org/pubservs/epaps.html.
[29] A. Alù and N. Engheta, Phys. Rev. Lett. **102**, 233901 (2009).